Comptes Rendus

Physique

Stéphane Brûlé and Sébastien Guenneau

Past, present and future of seismic metamaterials: experiments on soil dynamics, cloaking, large scale analogue computer and space–time modulations

Part of Special Issue: Metamaterials 2
Guest editors: Boris Gralak (CNRS, Institut Fresnel, Marseille, France)
and Sébastien Guenneau (UMI2004 Abraham de Moivre, CNRS-Imperial College,
London, UK)

CENTRE
MERSENNE

Metamaterials 2 / *Métamatériaux 2*

Past, present and future of seismic metamaterials: experiments on soil dynamics, cloaking, large scale analogue computer and space–time modulations

Passé, présent et futur des métamatériaux sismiques : expériences sur la dynamique des sols, camouflage, calculateur analogique à grande échelle et modulations spatio–temporelles

Stéphane Brûlé*, **ᵃ and Sébastien Guenneau ᵇ**

ᵃ Aix Marseille Univ, CNRS, Centrale Marseille, Institut Fresnel, Marseille, France

ᵇ UMI 2004 Abraham de Moivre-CNRS, Imperial College London, London SW7 2AZ, UK

E-mails: stephane.brule@menard-mail.com (S. Brûlé), s.guenneau@imperial.ac.uk (S. Guenneau)

Abstract. Some properties of electromagnetic metamaterials have been translated, using some wave analogies, to surface seismic wave control in sedimentary soils structured at the meter scale. Two large scale experiments performed in 2012 near the French cities of Grenoble [1] and Lyon [2] have confirmed the usefulness of this methodology and its potential influence on soil-structure interaction. We present here a new perspective on the in-situ experiment near Lyon, which unveils energy corridors in the seismic lens. We further introduce a concept of time-modulated seismic metamaterial underpinned by an effective model based on Willis's equations. As a first application, we propose that ambient seismic noise time-modulates structured soils that can be viewed as moving media. In the same spirit, a design of an analogous seismic computer is proposed making use of ambient seismic noise. We recall that ancient Roman theaters and forests of trees are two examples of large scale structures that behave in a way similar to electromagnetic metamaterials: invisibility cloaks and rainbows, respectively. Seismic metamaterials can thus not only be implemented for shielding, lensing and cloaking of potentially deleterious Rayleigh waves, but they also have potential applications in energy harvesting and analogous computations using ambient seismic noise, and this opens new vistas in seismic energy harvesting and conversion through the use of natural or artificial soil structuring.

---

* Corresponding author.

Résumé. Certaines propriétés des métamatériaux électromagnétiques ont été traduites, en utilisant certaines analogies d'ondes, en contrôle des ondes sismiques de surface dans des sols sédimentaires structurés à l'échelle du mètre. Deux expériences à grande échelle réalisées en 2012 près des villes françaises de Grenoble [1] et Lyon [2] ont confirmé l'utilité de cette méthodologie et son influence potentielle sur l'interaction sol-structure. Nous présentons ici une nouvelle perspective sur l'expérience in-situ menée près de Lyon, qui dévoile des couloirs d'énergie dans la lentille sismique. Nous introduisons en outre un concept de métamatériau sismique modulé dans le temps sous-tendu par un modèle effectif s'appuyant sur les équations de Willis. Dans une première application, nous proposons que le bruit sismique ambiant module dans le temps les sols structurés pouvant être considérés comme des milieux en mouvement. Dans le même esprit, il est proposé de concevoir un calculateur analogique sismique utilisant le bruit sismique ambiant. Nous rappelons que les anciens théâtres romains et les forêts d'arbres sont deux exemples de structures à grande échelle qui se comportent de manière similaire aux métamatériaux électromagnétiques : capes d'invisibilité et rainbows (anglicisme d'arcs-en-ciel), respectivement. Les métamatériaux sismiques peuvent donc non seulement être mis en œuvre pour des murailles, lentilles et capes pour ondes de Rayleigh potentiellement délétères, mais ils ont également des applications potentielles dans la récupération d'énergie et des ordinateurs analogiques utilisant le bruit sismique ambiant, ce qui ouvre de nouvelles perspectives dans la récupération et la conversion d'énergie sismique grâce à l'exploitation de structuration naturelle ou artificielle des sols.

Keywords. Seismic metamaterial, Transformational physics, Time-modulated medium, Homogenization, Analogue computer, Ambient seismic energy.

Mots-clés. Métamatériaux sismiques, Physique transformationnelle, Milieux modulés en temps, Homogénéisation, Calculateur analogique, Energie sismique ambiante.

1. Introduction

In earthquake engineering, the trapping of seismic waves in natural u-shaped basin filled with very soft sediments remains a major issue such as for Mexico City downtown built on a former drought lake [3]. Independently of the path taken by the body waves coming from the earthquakes focus located in the crust a few tens of kilometers deep, essential wave transformations occur in the last tens of meters below the free surface. Main effects are interaction between different components of body waves at the Earth's surface generating Rayleigh surface waves, strong wave magnitude amplification at the free surface (e.g. site effects), wave trapping prolonging the duration of the signal, and so forth. At the scale of the Earth, there is a clear differentiation of the seismic motion at the surface because of local and superficial geological features (shape of sediment layers, density contrasts, anisotropy, viscoelasticity effect, etc.). That is exactly what scientific research on wave physics and more precisely, on seismic metamaterials tries to anticipate, asserting that the creation of a small-volume of anisotropic ground, made of a 2D mesh of inclusions inside the bulk, can also induce seismic wave-matter interactions [1, 2, 4] with civil engineering purposes. The influence of such inclusions in the ground can be characterized in different, complementary, ways by numerical models and site-experiments: wave mode conversion, redistribution of energy within the network with focusing effects, wave reflection, frequency filtering, reduction of the amplitude of seismic signal energy, etc. In this article, we browse the main tools to design the smart deep infrastructure of tomorrow, presenting an introduction to the field of seismic metamaterials (Section 1), pointing out some analogous phenomena observed in the field of electromagnetic metamaterials, not only the now well established negative refraction, (Section 2) and cloaking (Section 3), but also large scale metamaterials analogues of computers solving integral equations making use of ambient seismic noise (Section 4) and finally some prediction of non-reciprocal effects for surface seismic waves akin to those in electromagnetic time-modulated media (Section 5) and bridging the two fields via the unifying concept of transformational optics and acoustics. Since the first in-situ experiment carried out in 2012 [1], many

research groupings worldwide have started to work on this topic, and although this field of seismic metamaterials is still in its infancy, we believe it has a bright future. One of the future perspectives we propose to initiate is an outline of a two-scale homogenization theory based on [5], that shows exotic effective elastodynamic media that can be achieved with soils structured with boreholes and concrete (or steel) columns. Indeed, we stress that Willis's equations [6], which have an additional term in the constitutive equation related to the gradient of pre-stresses, compared to classical constitutive equation of linear elasticity for homogeneous media, are a natural framework when a seismic wave passes through such structured soils. Interestingly, Willis's equations have a counterpart in electromagnetics, so-called bi-anisotropic equations with a magneto-optic coupling tensor [7], which have been recently shown to mimic moving media [8]. We finally propose to translate the concept of electromagnetic metamaterial analog computing [9, 10], based on suitably designed metamaterial cells that can perform mathematical operations (such as spatial differentiation, integration, or convolution) on the profile of an impinging wave as it propagates through these cells, to the realm of seismology. We will finally propose some new types of seismic metamaterials, that we coin as seismic computers. This bold idea is to make use of mechanical energy of small earthquakes which occur daily, to perform mathematical operations on a large scale at a minimum cost. We think this theoretical proposal of a kind of Türing machine at a geophysical scale can be a green contribution for our planet, since apart from the human-seismic machine interface, it does not require any energy consuming device to work. We further believe that using ambient noise at the Earth scale, a new type of world wide web could emerge, connecting seismic computers from various parts of the world. Finally, as a twist of epistemology, it looks like seismic metamaterials were already present in the ancient world, and we will say more about that in the sequel.

2. Revisiting the 2012 site-experiment in Saint-Priest

The wave trapping in a sedimentary basin may be the cause of phenomena of amplification of the seismic motion and prolongation of the duration of the shaking. The full-scale vibration experiments carried out in France during the year 2012 on two arrays of holes [1, 2] have shown the reality of the elastic wave-matter interaction for the case of artificial structured soils, just beneath the Earth's surface. Inside the grid of holes and for the near field, the distribution of the mechanical energy has been significantly modified. In this article, we propose to revisit the experience of Saint Priest (a small town located nearby the French city of Lyon) conducted in 2012 by presenting original results. So far we wanted to show the remarkable effective properties that could be obtained by structuring the soils (reflexion, negative refractive index, etc.) and try to identify what could be the link with earthquake engineering [11].

2.1. *Energetic seismic metamaterials*

However, we propose to open a complementary research track based on some observations on the turbulence of the velocity field inside a structured fluid, known as an invisibility carpet and demonstrated for water waves at a meter scale [12]. In this experimental study on the control of water waves within a 17 m long water channel, it was found that the velocity field was very disturbed inside the corridors of the water wave cloak. Similar observation was made twelve years ago on numerical simulations performed for a small scale experiment on a water wave invisibility cloak [13], see Figure 1. We have already pointed out the analogous behaviour of water waves in structured fluids, and Rayleigh waves in soft structured soils [14]. It seems thus possible that similar enhancement for the velocity field of the elastodynamic waves within the structured soil in Saint-Priest might occur, as this seismic metamaterial can be viewed as a transformed
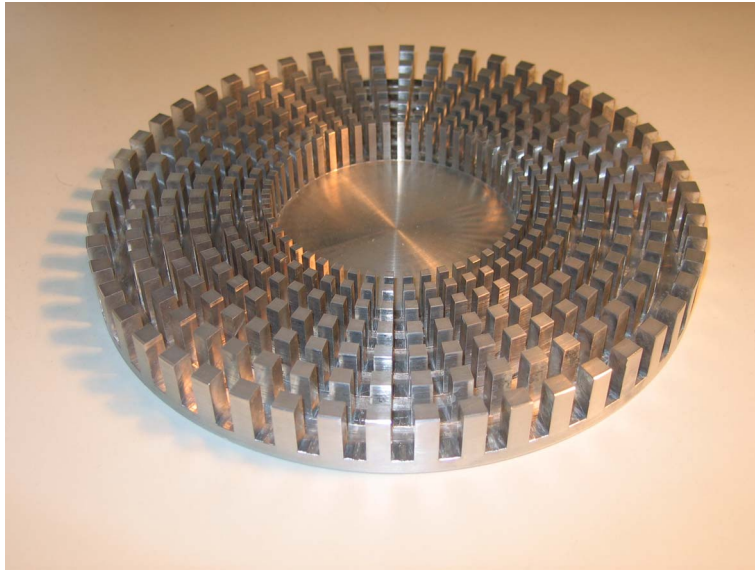
Figure 1. Photo (credit: S. Enoch) of the multi-wave metamaterial cloak (made of aluminium) designed, simulated, and experimentally tested at Institut Fresnel in 2008: this cloak which is 20 cm in diameter and 1 cm in height smoothly detours water waves around its center from 8 to 15 Hz. Cloaking is also achieved for micro waves from 3 to 7 GHz and for airborne pressure waves from 4 to 8 kHz. A single governing equation (Helmholtz equation) models all three types of waves propagating though this cloak [15]. The same geometry works for cloaking of flexural waves in a thin plate [16]. A scaled-up version of this cloak serves as an inspiration for designs of seismic cloaks at the meter scale.

medium [11], just like the carpet in [12] and the cloak in [13], and so all these metamaterials should share similar features.

Thus, one wonders whether the mechanical energy inside the seismic metamaterial is not a potential resource to exploit. The peak of particle velocity is a few mm·s^{-1} for the vibrations generated by urban work site—The amplitude of urban seismic noise ranges from 10^{-6} to 10^{-4} m·s^{-1}.

For the largest amplitudes of this range, with a mechanical energy conversion with calibrated buried oscillators, we can hope to light a bulb of a few tens of Watt. The answer is positive as we now show making use of existing data with measurements acquired inside the corridors of the Saint-Priest grid of holes, see Figure 2. We would like to coin such large scale structured seismic energetic metamaterials, since they have a purpose in energy harvesting [17]. We believe this subfield of seismic metamaterials might have a bright future.

This large scale experiment, which took place near the French city of Lyon in September 2012, is a large scale phononic crystal, made of five rows of self-stable boreholes 2 m in diameter, 5 m in depth with a center-to-center spacing of 7 m, see Figure 2. To capture the ground motion's field, a set of 15 three-component velocimeters (V_x, V_y, V_z) has been implemented on site. The sensors were used simultaneously with a common time base and were densely set on half of the grid. For the purposes of the study, here we present only the sensors inside the grid. The artificial source consisted this time of the fall of a 17 ton steel pounder from a height of about 12 m to generate clear transient vibrations pulses. We checked that most of the energy of the source was converted into energetic surface waves. The typical waveform of the source in time-domain looked like a
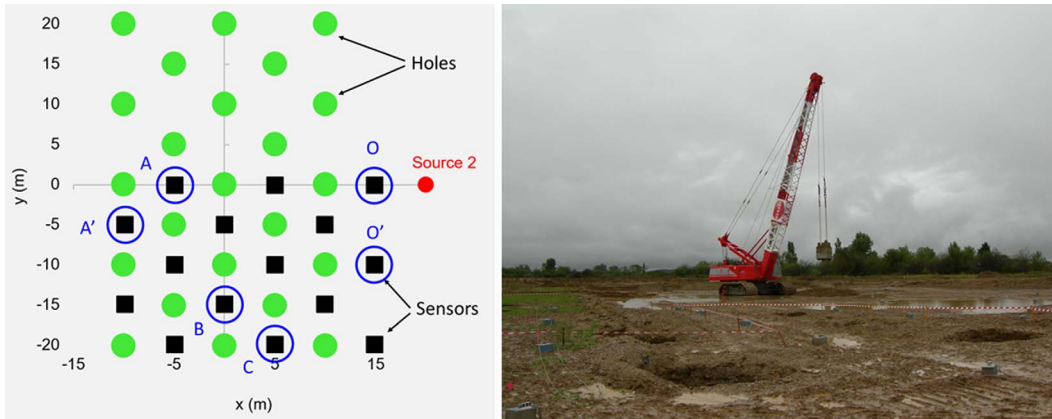
Figure 2. Experiment on a flat seismic lens: (Left) Plan view of field-site layout with 23 boreholes (green disks), 2 m in diameter, 5 m in depth, with hole spacing of 5 m. Sensors (black squares) are located midway between the holes, with 5 m spacing. The source (red disk) is located 10 m in horizontal distance from the first row of holes. Points A, A′, O, O′, B, C are sensors selected for the study of energy or frequency filtering effect, see Figures 4–5. (Right) Photo (credit: S. Brûlé) of the field experiment near the French city of Lyon in September 2012, with some boreholes in the foreground and a crane carrying a 17 ton mass (the seismic source) in the background.
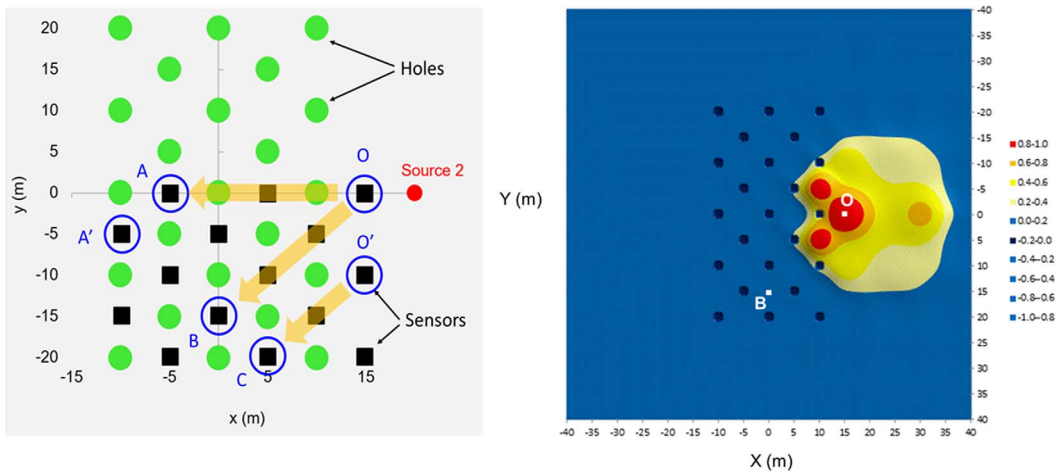
Figure 3. (Left) Selected corridors for the experimental study on frequency filtering and energy distribution: line 1 from point O to A, line 2 from point O to B and line 3 from O′ to C. (Right) Snapshot illustrating the recorded energy distribution in the soil structured with 23 holes after an impact (17 ton mass dropped for the crane shown in Figure 2) at the Earth's surface. Source is located at ($x = 20$, $y = 0$).

second order Ricker wavelet (or "Mexican hat wavelet"). The signal was characterized by a mean frequency value at 8.15 Hz ($\lambda_{P\text{-wave}} \sim 74$ m) with a range of frequencies going from 3 Hz to 20 Hz ($30 < \lambda_{P\text{-wave}} < 200$ m). A preliminary test was performed on the ground without holes with sensors arranged in a single row. Thereafter, we compare the measurements acquired on a soil without holes with those acquired inside the grid of holes.

The diagrams in Figure 5 show the decrease in energy with the distance from the source. The energy is defined as the sum of the squared value of each component (V_x, V_y, V_z) of the seismogram. With or without holes in the ground, the energy decreases very quickly with the distance. On the total energy diagram (Figure 5(a)), the energy decreases for the three profiles, but much less quickly on the first 15 m for OB (black dotted line) and O′C (grey dotted line). For the profile OA (solid black curve) passing through the holes, the decay is linear. We can advance two explanations to this observation. The first is a strong reflection of the seismic signal coming on the long side of the array. The second is a channelization of energy in the soil bridges between the holes. This phenomenon can be seen on a snapshot in time domain, showing the energy map inside the grid (Figure 3) and along the corridor OB.

Now, if we study the energy diagrams by components (V_x^2, V_y^2, V_z^2), we observe that the energy ratio between the different components is changing with the offset and with the corridor considered (Figure 3(b) and (c)). The OA profile shows an apparent regularity by component, but the ordinate scale being logarithmic the differences between components are nevertheless marked. At 15 m, there is an inversion of importance between the X and Z components (profile OA). These rapid changes seem to reflect changes in polarization of the seismic signal [18]. Let's see if we can explain this in the spectral domain. We have calculated the magnitude in dB of three transfer functions $|T_x(\omega)|$, $|T_y(\omega)|$ and $|T_z(\omega)|$ as the spectral ratio of the ground particle velocity for a couple of sensors (O, A) and (O, B). Basically we considered the grid of holes as a filter without any consideration of initial soil properties (wave velocity, pattern of the grid, etc.).

$$|T_{A/O}(\omega)| = |\mathscr{A}(\omega)/\mathscr{O}(\omega)| \tag{1}$$

with $\mathscr{A}(\omega)$ and $\mathscr{O}(\omega)$ the Fourier transforms of signal recorded with sensor A and O.

The transfer function represents information relating to the signal entering in the grid of holes (point A or B) from the right-hand side of the Figure (point O or O′). We have calculated the magnitude in dB of the transfer function for the initial soil (solid blue line) and for the structured soil with holes (solid red line). We have also drawn the magnitude of the original soil transfer function minus 3 dB (gray dotted line) to illustrate the efficiency of the holey-ground. We consider that results acquired with the land streamer (solid blue line) make the benchmark curve to compare with the others. It is the spectral signature of the soil with its initial peculiarities. $T_{A/O}$ and $T_{B/O}$ curves are significantly different. For $T_{A/O}$ in the left hand side of Figure 4, we observe an horizontal amplification of the particle's velocity (solid red line), compared to the ground without hole (blue solid line), from 1 to 10 Hz. For the vertical component, the amplification is identified between 1 and 2 Hz and 4 and 10 Hz. Between 2 and 4 Hz, there is a de-amplification of the magnitude around 3 dB (grey dotted line).

In regards to $T_{B/O}$ curves, only de-amplification from 1 to 10 Hz is observed for x-component, after completion of the holes. Same observation up to 2.3 Hz for the y-component but then, there is amplification unlike what was described for x-component. For the y-component, there is only amplification between 4.6 and 10 Hz with a peak at 6.5 Hz. Overall, there is a larger frequency bandwidth regarding de-amplification for the profile passing between the holes (OB) than for the line crossing the holes (OA). Roughly speaking, the signal is much more attenuated horizontally in x and vertically in z and for a broader range of frequency for the profile passing between the holes (OB) than for the line crossing the holes (OA). However, there is amplification according to y. These contrasts between $T_{A/O}$ and $T_{B/O}$ result in polarization changes for the seismic waves, as further discussed in terms of dynamic effective properties akin to auxetic media (with a negative Poisson ratio) in [3]. We believe that the realization of holes and the associated densification of soils might be the cause of the 6.5 Hz peak in z-component. Also worth mentioning is that we have proposed here a viewpoint in the context of linearized elastic wave equations, but some
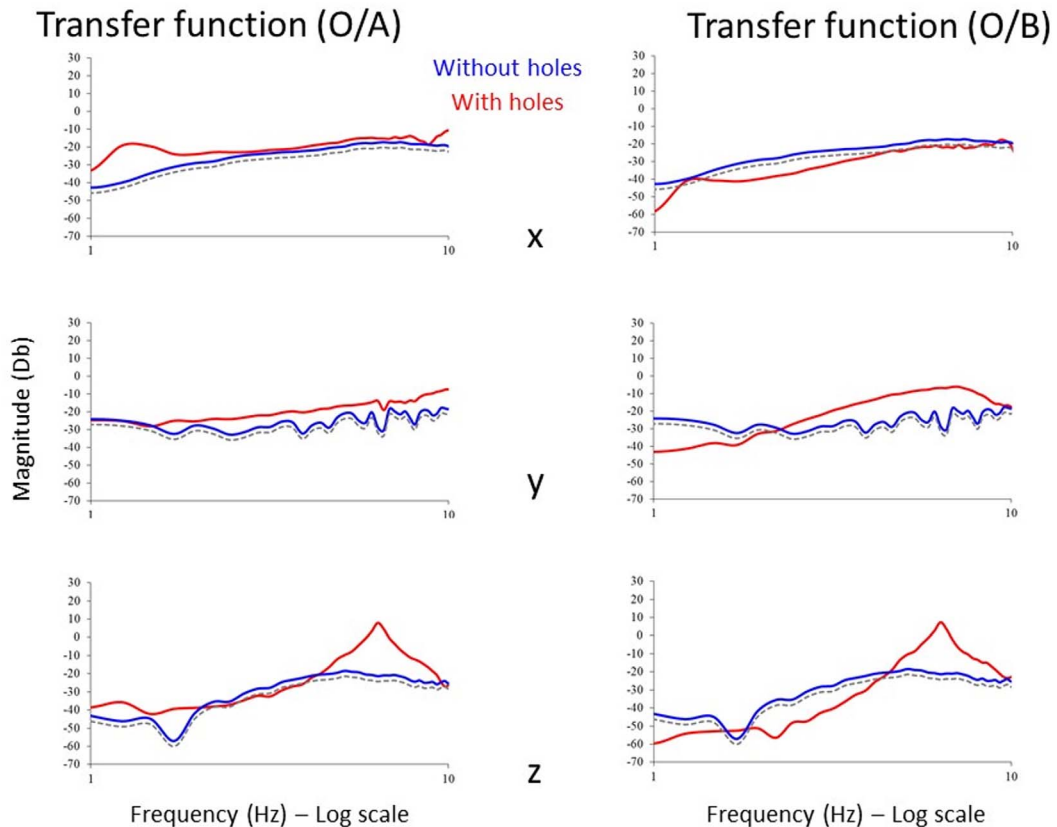
Figure 4. Transfer functions O/A and O/B for *x* (upper panel), *y* (middle panel) and *z* (lower panel) component of two velocimeters located inside the array of boreholes, compared to those of a velocimter placed in between the source and the array, as shown in Figure 1(left). (OA) is for the line passing through the source and the two circled sensors. (OB) is for the line passing through a corridor without boreholes, see Figure 3. Light blue curves are for soil without holes and red curves for structured soil.

interesting non-linear effects would be also woth studying such as the possibility of rogue waves in soft soils that one could counteract with the array of boreholes [19].

3. Seismic cloaks, Roman theaters and forests of trees

On the basis of these results, we extend the theoretical analysis to ancient structures, made up of many elements of symmetries such as the foundations of Roman amphitheatres [4].

3.1. *Seismic metamaterials from the ancient world*

Built of travertine, tuff, and brick-faced concrete, the Coliseum in Roma is the largest amphitheatre ever built. Construction began under the emperor Vespasian in AD 72 and was completed in AD 80 under his successor and heir, Titus. A numerical simulation was conducted on a structured soil reproducing the geometry of the foundations of an ancient amphitheater (see Figure 6(b)), with a source inside (see Figure 6(c)) and outside (see Figure 6(d)) of the structure. The similarity
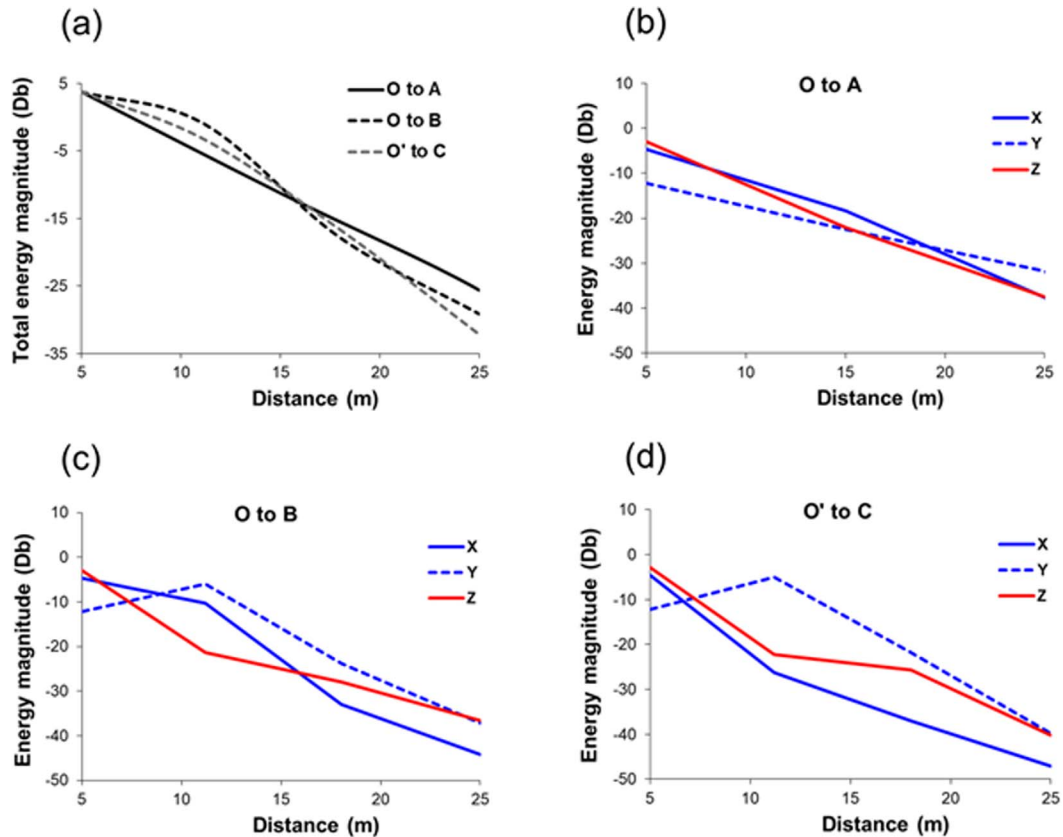
Figure 5. Mechanical energy magnitude versus offset, according to the studied corridor. (a) Total energy mesured for the three selected corridors (O to A, O to B and O′ to C). Diagrams (b), (c) and (d) show respectively the energy by component X, Y, Z versus offset, for corridors OA, OB et O′C shown in Figure 3.

between the foundations of the Coliseum in Figure 6(b) and the design of the invisibility cloak in Figure 1 can be seen in Figure 6(a). We note that such fortuitous seismic metamaterials could inspire seismic cloak designs at the scale of cities [20].

3.2. *Forests as seismic metamaterials*

There is currently a renewed interest in site-city interactions as slender bodies such as medium size buildings placed atop of soft soil may have a strong interaction with surface seismic waves in the 1 to 10 Hz frequency range. This has been further explored in a recent work [4]. It has been recently proposed that other types of locally resonant large scale structures such as forest of trees can shield [21] and convert [22] surface Rayleigh waves. The latter can be viewed as an elastic counterpart of graded metamaterial surfaces in electromagnetics, that make possible a rainbow effect whereby the colors of light are filtered by resonant elements of varying sizes [23]. This type of rainbow effect has been also noted for Love waves propagating in soils with a soft guiding layer surmounted by a forest of trees, see Figure 7 in which case a complete correspondence with spoof plasmon polaritons has been mathematically established [24]. Interestingly, it has
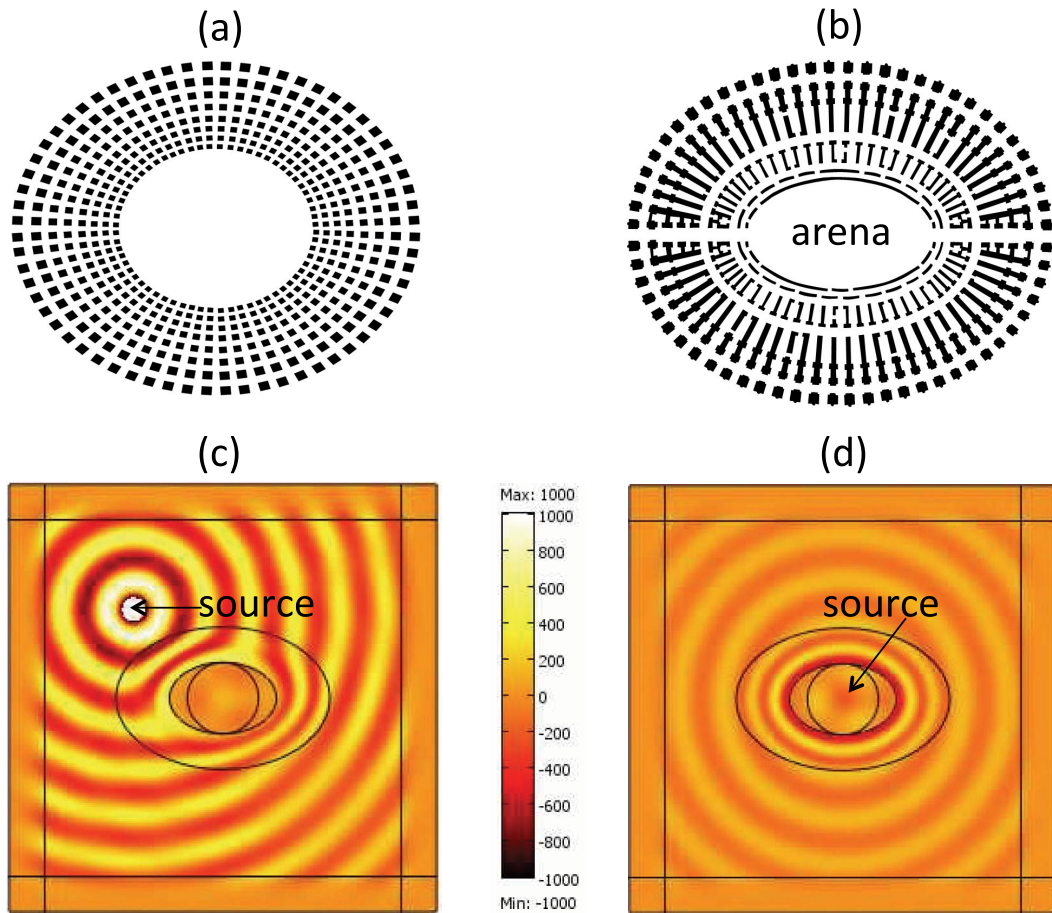
Figure 6. The Coliseum: an unexpected seismic metamaterial from the ancient world. (a) Geometry of the cloak in Figure 1 mapped onto an ellipsis. (b) Geometry of the Coliseum Main axes of arena are 86 m by 54 m (height of 4.5 m) and outer dimensions are 187.75 m by 155.60 m (height of 50.75 m). (c) Finite element (Comsol) simulation for a flexural wave, emitted by a point source of wavelength 35 m, propagating in an elastic plate (of thickness 3 m) with an elliptical cloak with similar dimensions to the Coliseum. (d) Same for a source located inside the arena. One notes the reduced amplitude of field in arena in (c) and its enhancement at the boundary of arena in (d).

been demonstrated in [25] that one can design special types of elastic rainbows that can harvest Rayleigh waves and we believe a similar design can be applied to harvest Love waves.

After this review of seismic metamaterials from the past and the present, we would like to turn our mind to seismic metamaterials of the future.

4. Proposal for an analogue computer with a seismic metamaterial

Before we detail our proposal for a seismic computer, we need to recall the main difference between analogue and digital computers. An analogue computer is a type of computer that relies on the continuously changeable aspects of physical phenomena such as electrical, mechanical,
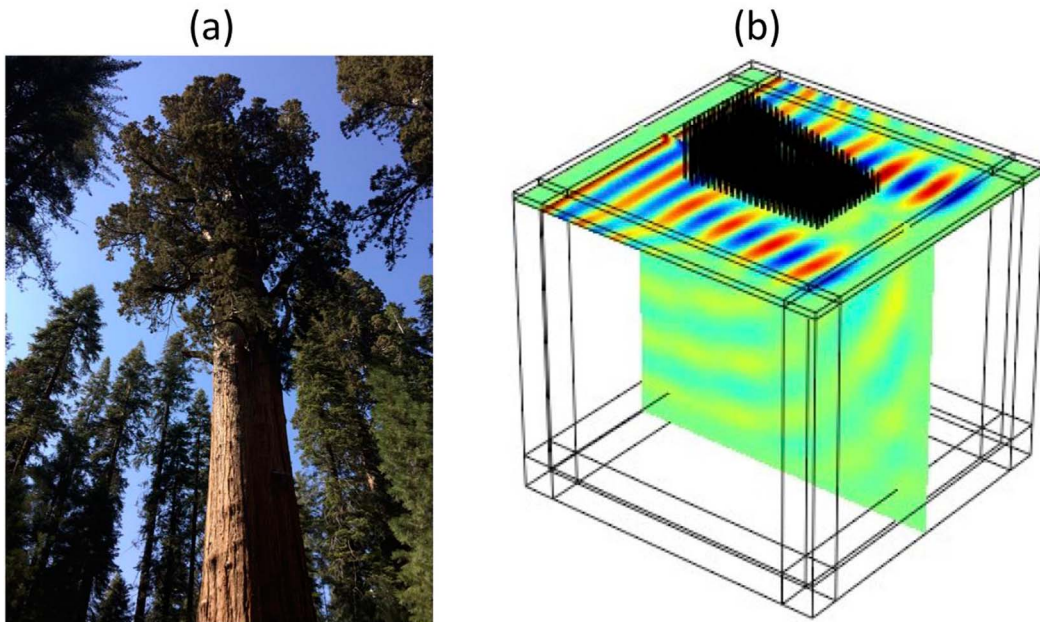
Figure 7. Forests as seismic metamaterials: (a) Photo (S. Brule) of the General Sherman (height of 83.7 m, diameter of 7.7 m) which is located in California's Sequoia National Park. (b) Finite element (Comsol) simulation of a Love wave of frequency 10 Hz propagating through a forest of tree trunks (without foliage) of heights ranging from 80 m to 4 m. When adding foliage to the tree trunks, same effect can occur for a Love wave of frequency 5 Hz (or alternatively at 10 Hz for trees twice as small), according to a theory developed in [24].

or hydraulic quantities to model the problem being solved. In contrast, digital computers represent varying quantities symbolically, as their numerical values change. As an analogue computer does not use discrete values, but rather continuous values, processes cannot be reliably repeated with exact equivalence, as they can with Türing machines. Unlike machines used for digital signal processing, analogue computers do not suffer from the discrete error caused by quantisation noise. Instead, results from analog computers are subject to continuous error caused by electronic noise. We now wish to propose an analogue computer that would use the energy of ambient seismic noise in structured sedimentary soils. Mechanical analogue computing devices date back at least to the Roman author, architect civil and military engineer Marcus Vitruvius Pollio who lived in the first century BC, who is known for his multi-volume work entitled De architectura [26]. His discussion of perfect proportion in architecture and the human body led to the famous Renaissance drawing by Leonardo da Vinci of Vitruvian Man which describes the use of a wheel for measuring an arc length along a curve i.e. the most simple integral in space. Many other elementary analogue devices were described until now, see for instance [27].

We shall only recall here that James Clerk Maxwell described a ball type of integrating device while he was an undergraduate: it was incorporated in a planimeter design, which is a measuring instrument used to determine the area of an arbitrary two-dimensional shape.

We propose that metastructures hold the potential to bring a new twist to the field of spatial-domain optical analogue computing: migrating from conceptually wavelength-sized elements for electromagnetic waves to seismic waves. We show in Figure 8 the principle of a metamaterial soil capable of solving integral equations using ambient seismic noise. For an arbitrary seis-

mic wave as the input function to an equation associated with a prescribed integral operator, the solution of such an equation is generated as a complex-valued output seismic field. Our approach is based on analogies drawn with the seminal work [10] which experimentally demonstrated the concept of an analogue optical computer at microwave frequencies through solving a generic integral equation and using a set of waveguides as the input and output to the designed metastructures. By exploiting subwavelength-scale light-matter interactions in a metamaterial platform, the analogue computer may provide a route to achieve chip-scale, fast, and integrable computing elements. The researchers believed metamaterials could offer several important advantages over this conventional digital process. One benefit is that the computational process could be extremely fast because electromagnetic waves pass through metamaterials at the speed of light. Also, the same metamaterial can process multiple waves simultaneously. In the present case, the emphasis is on decameter scale seismic analogue computers that could solve complex mathematical equations using natural resources (ambient seismic noise). The seismic metamaterial analogue computer should be based on metamaterial blocks that can perform mathematical operations (such as spatial differentiation, integration, or convolution) on the profile of a surface (Rayleigh and Love) and bulk (shear and pressure) seismic waves as they propagate through these blocks. Two types of seismic metamaterials can achieve such functionality: (i) subwavelength structured metascreens combined with graded-index seismic waveguides such as forest of trees in Figure 7 and multilayered soils designed to achieve a desired spatial Green's function such as in Figure 8. Our proposal for these two types of seismic computers will require further theoretical and experimental efforts to become a tangible reality, but we are confident that at least one of the two routes towards of seismic computer can be tested in the near future.

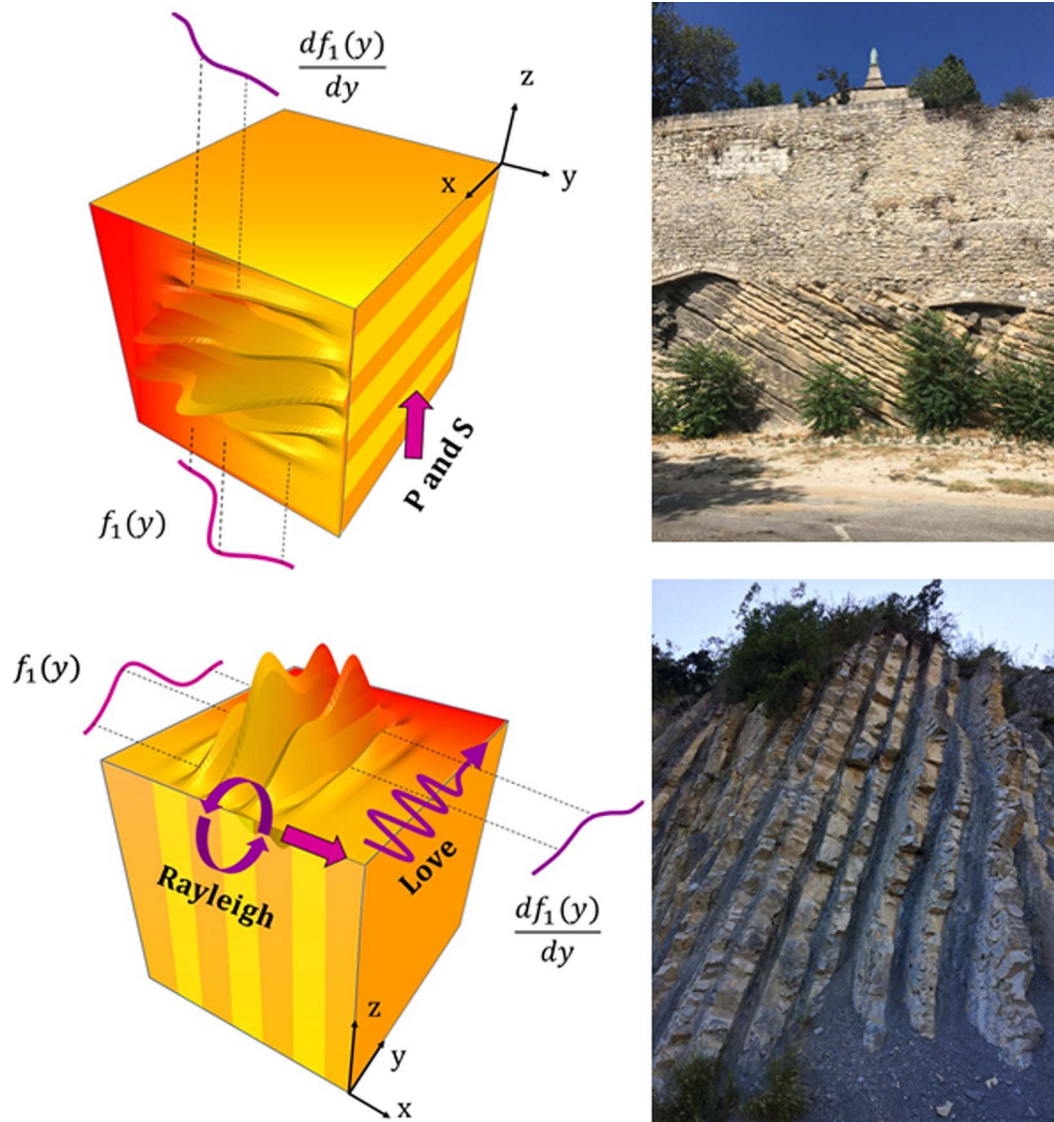## 5. Seismic metamaterials versus space–time modulated media

There is currently a keen interest in space–time modulated media in optics, as these can be mapped onto bi-anisotropic equations in the long wavelength limit, which present interesting features such as non-reciprocity of light propagation in moving media [8]. We propose here to adapt these results to surface seismic waves propagating in a vibrating soil, which can then be modelled as Willis' equations in the long wavelength limit as we will now show using the approach of [5]. We further note that homogenization results derived in [5] for the elastic wave equation, are an extension of results obtained in [28] for the acoustic wave equation. The latter is a very comprehensive, and landmark, textbook on the topic of dynamic materials, which are nothing but consecrated space–time mdulated media. We stress that the time-modulated system studied in [5] is a good model for the seismic computer that we study here.

5.1. *Two-scale homogenization of the modulated vector Navier system*

We consider the two-scale homogenization of the vector Navier system of a time-modulated layered medium. For this we need a fixed space–time Cartesian coordinate system $(\mathbf{x}, t) = (x_1, x_2, x_3, t)$ and a time modulated layered periodic medium. The propagation is assumed along the direction x_1 of stacking of layers. In what follows, the subscript denotes dependence of the field upon the periodicity η in the space–time variable $x_1 - c_1 t$, where c_1 is the modulation speed along x_1. We mostly follow the same lines as the derivation of Nassar et al. [5]. One considers a displacement field $\mathbf{A}_\eta$ which is a function on $\mathbb{R}^3 \times [0, T]$ solution of

$$(\mathscr{P}_\eta^{\mathbf{A}}) \begin{cases} \nabla \cdot \left[\tilde{\mathbf{C}}\left(\mathbf{x}, t, \frac{x_1 - c_1 t}{\eta}\right) : \nabla \mathbf{A}_\eta \right] = \frac{1}{c^2} \frac{\partial}{\partial t} \left[\tilde{\rho}\left(\mathbf{x}, t, \frac{x_1 - c_1 t}{\eta}\right) \frac{\partial}{\partial t} \mathbf{A}_\eta \right], \\ \mathbf{A}_\eta(\mathbf{x}, 0) = \overline{\mathbf{A}}_\eta(\mathbf{x}), \end{cases}$$

Figure 8. Principle of the seismic computer: sketch of suitably designed (Left) and naturally occuring (Right) layered soils that may perform a desired mathematical operation (e.g. integration and differentiation) on arbitrary seismic wave signals (ambient noise) in the case of volume pressure (P) and shear (S) waves (Top), and surface Love and Rayleigh waves (Bottom), as they propagate through it (adapted from [10]). (Upper left) Photo of inclined geologic layers with horizontal rows of stone walls in Arles, France (credit: S. Brûlé). (Lower right) Photo of subvertical geological layers with a regular alternation (with periodicity of about 1 m) of limestones (yellow) and marl (dark) in La Charce, France (credit: S. Brûlé).

where $\tilde{\mathbf{C}}(\mathbf{x}, t, (x_1 - c_1 t)/\eta)$ and $\tilde{\rho}(\mathbf{x}, t, (x_1 - c_1 t)/\eta)$ respectively denote the rank-4 elasticity tensor and density which are equal to $\mathbf{C}((x_1 - c_1 t)/\eta)$ and $\rho((x_1 - c_1 t)/\eta)$ in the modulated layered medium that is in the interval $x_1 \in [0, h]$ and $\mathbf{C}_0$ and ρ_0 outside the layered time-modulated soil. These parameters are 1 periodic functions of x_1 and $1/c_1$ periodic functions of t.

From now on we assume that $\mathbf{C}_0 = \mathbf{I}$ and $\rho_0 = 1$ using the linearity of the Navier system, and we consider the following ansatz for the vector displacement field

$$\mathbf{A}_\eta(\mathbf{x}, t) = \mathbf{A}_0\left(\mathbf{x}, t, \frac{x_1 - c_1 t}{\eta}\right) + \eta \mathbf{A}_1\left(\mathbf{x}, t, \frac{x_1 - c_1 t}{\eta}\right)$$
$$+ \eta^2 \mathbf{A}_2\left(\mathbf{x}, t, \frac{x - c_1 t}{\eta}\right) + \cdots \tag{2}$$

where $\mathbf{A}_i : [0, h] \times \mathbb{R} \times \mathbb{R} \times [0, T] \times Y \longmapsto \mathbb{C}^3$ is a smooth vector valued function of 5 variables, independent of η, such that $\forall (\mathbf{x}, t) \in [0, h] \times \mathbb{R} \times \mathbb{R} \times [0, T]$, $\mathbf{A}_i(\mathbf{x}, t, \cdot)$ is 1-periodic in $\mathbb{R}$.

We consider the coordinate system $(y, t) = (x_1 - c_1 t, t)$, in the moving frame attached to the modulated medium. We note that the partial derivatives in the moving frame can be expressed as $(\partial_{x_1}, \partial_t) = (\partial_y, -c_1 \partial_y + \partial_t)$. In a way similar to what is usually done for homogenization of unmodulated periodic media we replace the partial differential operator acting on the space variable x_1 by the two-scale operator $\partial/\partial x_1 := \partial/\partial x_1 + (1/\eta)(\partial/\partial y)$, and thus the rescaled curl operator can be expressed as

$$\nabla = \nabla + \left(\frac{\partial}{\eta \partial y}, 0, 0\right)^T = \left(\nabla + \frac{\mathbf{n}}{\eta}\frac{\partial}{\partial y}\right), \tag{3}$$

where $\nabla = (\partial/\partial x_1, \partial/\partial x_2, \partial/\partial x_3)^T$ and $\mathbf{n}$ is the unit outward normal to the layers's interfaces. Moreover we do the same for the partial differential operator acting on the time variable t, so that $\partial/\partial t := \partial/\partial t - (c_1/\eta)(\partial/\partial y)$. These two-scale operators are combined with the asymptotic expansion of the potential field $\mathbf{A}_\eta$.

Assuming that the terms of the development of the powers higher than 2 are bounded in (2), we can write:

$$\left[\nabla + \frac{\mathbf{n}}{\eta}\frac{\partial}{\partial y}\right] \cdot \left(\tilde{\mathbf{C}}(\mathbf{x}, t, y) : \left[\nabla + \frac{\mathbf{n}}{\eta}\frac{\partial}{\partial y}\right](\mathbf{A}_0 + \eta \mathbf{A}_1 + \eta^2 \mathbf{A}_2)\right)$$
$$= \nabla \cdot \left(\tilde{\mathbf{C}} : \nabla(\mathbf{A}_0 + \eta \mathbf{A}_1 + \eta^2 \mathbf{A}_2)\right) + \nabla \cdot \left(\tilde{\mathbf{C}} : \frac{\mathbf{n}}{\eta}\frac{\partial}{\partial y}(\mathbf{A}_0 + \eta \mathbf{A}_1 + \eta^2 \mathbf{A}_2)\right)$$
$$+ \frac{\mathbf{n}}{\eta}\frac{\partial}{\partial y}\left(\tilde{\mathbf{C}} : \nabla(\mathbf{A}_0 + \eta \mathbf{A}_1 + \eta^2 \mathbf{A}_2)\right)$$
$$+ \frac{\mathbf{n}}{\eta}\frac{\partial}{\partial y} \cdot \left(\tilde{\mathbf{C}} : \frac{\mathbf{n}}{\eta}\frac{\partial}{\partial y}(\mathbf{A}_0 + \eta \mathbf{A}_1 + \eta^2 \mathbf{A}_2)\right) + o(\eta)$$
$$= \left(\frac{\partial}{\partial t} - \frac{c_1}{\eta}\frac{\partial}{\partial y}\right)\left[\tilde{\rho}(\mathbf{x}, t, y)\left(\frac{\partial}{\partial t} - \frac{c_1}{\eta}\frac{\partial}{\partial y}\right)(\mathbf{A}_0 + \eta \mathbf{A}_1 + \eta^2 \mathbf{A}_2)\right] + o(\eta)$$
$$= \frac{\partial}{\partial t}\left[\tilde{\rho}\frac{\partial}{\partial t}(\mathbf{A}_0 + \eta \mathbf{A}_1 + \eta^2 \mathbf{A}_2)\right] - \frac{c_1}{\eta}\frac{\partial}{\partial t}\left[\tilde{\rho}\frac{\partial}{\partial y}(\mathbf{A}_0 + \eta \mathbf{A}_1 + \eta^2 \mathbf{A}_2)\right]$$
$$- \frac{c_1}{\eta}\frac{\partial}{\partial y}\left[\tilde{\rho}\frac{\partial}{\partial t}(\mathbf{A}_0 + \eta \mathbf{A}_1 + \eta^2 \mathbf{A}_2)\right] + \frac{c_1^2}{\eta^2}\frac{\partial}{\partial y}\left[\tilde{\rho}\frac{\partial}{\partial y}(\mathbf{A}_0 + \eta \mathbf{A}_1 + \eta^2 \mathbf{A}_2)\right] + o(\eta) \tag{4}$$

which leads to

$$\eta^{-2}\left[\mathbf{n}\frac{\partial}{\partial y} \cdot \left(\tilde{\mathbf{C}} : \mathbf{n}\frac{\partial}{\partial y}\mathbf{A}_0\right) - c_1^2\frac{\partial}{\partial y}\tilde{\rho}\frac{\partial}{\partial y}\mathbf{A}_0\right]$$
$$+ \eta^{-1}\left[\mathbf{n}\frac{\partial}{\partial y} \cdot (\tilde{\mathbf{C}} : \nabla\mathbf{A}_0) + \nabla \cdot \left(\tilde{\mathbf{C}} : \mathbf{n}\frac{\partial}{\partial y}\mathbf{A}_0\right) + \mathbf{n}\frac{\partial}{\partial y} \cdot \left(\tilde{\mathbf{C}} : \mathbf{n}\frac{\partial}{\partial y}\mathbf{A}_1\right)\right.$$
$$\left. - c_1^2\frac{\partial}{\partial y}\tilde{\rho}\frac{\partial}{\partial y}\mathbf{A}_1 + c_1\frac{\partial}{\partial y}\tilde{\rho}\frac{\partial}{\partial t}\mathbf{A}_0 + c_1\frac{\partial}{\partial t}\tilde{\rho}\frac{\partial}{\partial y}\mathbf{A}_0\right]$$
$$+ \eta^0\left[\nabla \cdot (\tilde{\mathbf{C}} : \nabla\mathbf{A}_0) + \nabla \cdot \left(\tilde{\mathbf{C}} : \mathbf{n}\frac{\partial}{\partial y}\mathbf{A}_1\right) + \mathbf{n}\frac{\partial}{\partial y} \cdot (\tilde{\mathbf{C}} : \nabla\mathbf{A}_1)\right.$$
$$\left. + \mathbf{n}\frac{\partial}{\partial y} \cdot \left(\tilde{\mathbf{C}} : \mathbf{n}\frac{\partial}{\partial y}\mathbf{A}_2\right) - \frac{\partial}{\partial t}\tilde{\rho}\frac{\partial}{\partial t}\mathbf{A}_0 - c_1^2\frac{\partial}{\partial y}\tilde{\rho}\frac{\partial}{\partial y}\mathbf{A}_2 + c_1\frac{\partial}{\partial y}\tilde{\rho}\frac{\partial}{\partial t}\mathbf{A}_1 + c_1\frac{\partial}{\partial t}\tilde{\rho}\frac{\partial}{\partial y}\mathbf{A}_1\right] = o(\eta). \tag{5}$$

In a neighborhood of $\eta = 0$, we express the vanishing of the coefficients of successive powers of $1/\eta$ which leads to three equations.

5.2. *What we learn from the order η^{-2}*

Let us start by the expression factor of η^{-2}, we obtain

$$\mathbf{n}\frac{\partial}{\partial y}\cdot\left(\tilde{\mathbf{C}}(\mathbf{x},t,y):\mathbf{n}\frac{\partial}{\partial y}\mathbf{A}_0\right) = c_1^2\frac{\partial}{\partial y}\tilde{\rho}(\mathbf{x},t,y)\frac{\partial}{\partial y}\mathbf{A}_0. \tag{6}$$

By integration over the periodic cell Y, we get

$$\left(\mathbf{n}\cdot\tilde{\mathbf{C}}(\mathbf{x},t,y)\cdot\mathbf{n} - c_1^2\tilde{\rho}(\mathbf{x},t,y)\mathbf{I}\right)\frac{\partial}{\partial y}\mathbf{A}_0(\mathbf{x},t,y) = \mathbf{m}(\mathbf{x},t) \tag{7}$$

where $\mathbf{I}$ is the rank-2 identity tensor and $\mathbf{m}$ is an integration (vector valued) function, so that integrating again over the periodic cell and taking into account that $\mathbf{A}_0$, $\tilde{\mathbf{C}}(\mathbf{x},t,y)$ and $\tilde{\rho}(\mathbf{x},t,y)$ are 1-periodic in y, we get

$$\mathbf{m}(\mathbf{x},t)\int_0^1 \mathrm{d}y = \mathbf{0} = \int_0^1 \left(\mathbf{n}\cdot\tilde{\mathbf{C}}(\mathbf{x},t,y)\cdot\mathbf{n} - c_1^2\tilde{\rho}(\mathbf{x},t,y)\mathbf{I}\right)\frac{\partial}{\partial y}\mathbf{A}_0(\mathbf{x},t,y)\,\mathrm{d}y. \tag{8}$$

Assuming that $\mathbf{n}\cdot\tilde{\mathbf{C}}\cdot\mathbf{n} - c_1^2\tilde{\rho}\mathbf{I}$, is a rank-2 tensor which is always definite positive or definite negative for $y\in[0,1]$, we deduce that

$$\frac{\partial}{\partial y}\mathbf{A}_0(\mathbf{x},t,y) = \mathbf{0} \tag{9}$$

which is just like the modulated elastic case in [5] for which one has that the leading order term in the asymptotic expansion of the displacement field (2), does not depend upon y.

5.3. *What we learn from the order η^{-1}*

Let us now look at the expression factor of η^{-1}, we have

$$\mathbf{n}\frac{\partial}{\partial y}\cdot(\tilde{\mathbf{C}}:\nabla\mathbf{A}_0) + \nabla\cdot\left(\tilde{\mathbf{C}}:\mathbf{n}\frac{\partial}{\partial y}\mathbf{A}_0\right) + \mathbf{n}\frac{\partial}{\partial y}\cdot\left(\tilde{\mathbf{C}}:\mathbf{n}\frac{\partial}{\partial y}\mathbf{A}_1\right)$$
$$- c_1^2\frac{\partial}{\partial y}\tilde{\rho}\frac{\partial}{\partial y}\mathbf{A}_1 + c_1\frac{\partial}{\partial y}\tilde{\rho}\frac{\partial}{\partial t}\mathbf{A}_0 + c_1\frac{\partial}{\partial t}\tilde{\rho}\frac{\partial}{\partial y}\mathbf{A}_0 = \mathbf{0}. \tag{10}$$

Using that $\mathbf{A}_0$ is independent of y, and assuming that we are at all times in the layered modulated medium $\tilde{\mathbf{C}}(\mathbf{x},t,y) = \mathbf{C}(y)$ and $\tilde{\rho}(\mathbf{x},t,y) = \rho(y)$, we obtain

$$\mathbf{n}\frac{\partial}{\partial y}\cdot\left(\mathbf{C}(y):\nabla\mathbf{A}_0\right) + \mathbf{n}\frac{\partial}{\partial y}\cdot\left(\mathbf{C}(y):\mathbf{n}\frac{\partial}{\partial y}\mathbf{A}_1\right)$$
$$+ c_1^2\frac{\partial}{\partial y}\rho(y)\frac{\partial}{\partial y}\mathbf{A}_1 - c_1\frac{\partial}{\partial y}\rho(y)\frac{\partial}{\partial t}\mathbf{A}_0 = \mathbf{0}. \tag{11}$$

Let us integrate over the periodic cell Y, we get

$$\frac{\partial}{\partial y}\mathbf{A}_1 = \mathbf{M}(y)\left(-\mathbf{n}\cdot\mathbf{C}(y):\nabla\mathbf{A}_0 - c_1\rho(y)\frac{\partial}{\partial t}\mathbf{A}_0 + \mathbf{p}\right), \tag{12}$$

where $\mathbf{p}$ is an integration vector and $\mathbf{M}(y) = (\mathbf{n}\cdot\mathbf{C}\cdot\mathbf{n} - c_1^2\mathbf{I})^{-1}$ is a symmetric, definite positive or negative rank-2 tensor.

Integrating once again over the periodic cell, we get

$$\int_0^1 \frac{\partial}{\partial y}\mathbf{A}_1\,\mathrm{d}y = \mathbf{0} = \int_0^1 (-\mathbf{M}(y)\otimes\mathbf{n}:\mathbf{C}(y)\,\mathrm{d}y):\nabla\mathbf{A}_0$$
$$+ c_1\int_0^1 (\mathbf{M}(y)\rho(y)\,\mathrm{d}y)\frac{\partial}{\partial t}\mathbf{A}_0 + \int_0^1 \mathbf{M}(y)\mathbf{p}\,\mathrm{d}y. \tag{13}$$

Combining (12) and (13), we get the following annex problem on the periodic cell

$$\frac{\partial}{\partial y}\mathbf{A}_1 = \mathbf{N}(y) : \nabla \mathbf{A}_0 + \mathbf{P}(y) \cdot \frac{\partial}{\partial t}\mathbf{A}_0, \tag{14}$$

where the tensors $\mathbf{N}(y)$ and $\mathbf{P}(y)$ are given by

$$\mathbf{N}(y) = \mathbf{M}(y)\left(\left(\int_0^1 \mathbf{M}(y)\,\mathrm{d}y\right)^{-1}\left(\int_0^1 (\mathbf{M}(y) \otimes \mathbf{n} : \mathbf{C}(y))\,\mathrm{d}y\right) - \mathbf{n} \cdot \mathbf{C}\right)$$

$$\mathbf{P}(y) = c_1 \mathbf{M}(y)\left(\left(\int_0^1 \mathbf{M}(y)\,\mathrm{d}y\right)^{-1}\int_0^1 (\mathbf{M}(y)\rho(y))\,\mathrm{d}y - \rho(y)\mathbf{I}\right). \tag{15}$$

5.4. *What we learn from the order η^0*

Finally, we look at the expression factor of η^0, performing an integration over the periodic cell, we obtain the homogenized equation of motion

$$\nabla \cdot \left(\int_0^1 \tilde{\mathbf{C}} : \left(\mathbf{n}\frac{\partial}{\partial y}\,\mathrm{d}y\mathbf{A}_1 + \nabla \mathbf{A}_0\right)\right)$$

$$= \frac{\partial}{\partial t}\int_0^1 \tilde{\rho}\frac{\partial}{\partial t}\mathbf{A}_0\,\mathrm{d}y - c_1\int_0^1 \frac{\partial}{\partial y}\tilde{\rho}\frac{\partial}{\partial t}\mathbf{A}_1\,\mathrm{d}y \tag{16}$$

which has the form of the equation $\nabla \cdot \Sigma = \partial_t \Pi$ where Σ is the macroscopic stress field and Π is the macroscopic momentum field.

The homogenized constitutive equations are, as first derived in [5],

$$\Sigma = \mathbf{C}_{\mathrm{eff}} : \nabla \mathbf{A}_0 + \mathbf{S}_{\mathrm{eff}}^1 \cdot \frac{\partial}{\partial t}\mathbf{A}_0$$

$$\Pi = \mathbf{S}_{\mathrm{eff}}^2 : \nabla \mathbf{A}_0 + \rho_{\mathrm{eff}} \cdot \frac{\partial}{\partial t}\mathbf{A}_0 \tag{17}$$

where the rank-4 homogenized elasticity tensor $\mathbf{C}_{\mathrm{eff}}$, the rank-3 homogenized coupling Willis tensors $\mathbf{S}_{\mathrm{eff}}^1$ and $\mathbf{S}_{\mathrm{eff}}^2$ and the rank-2 homogenized density tensor are given by:

$$\mathbf{C}_{\mathrm{eff}} = \langle \mathbf{C}\rangle + \langle \mathbf{C} : \mathbf{n} \otimes \mathbf{M}\rangle \cdot \langle \mathbf{M}\rangle^{-1} \cdot \langle \mathbf{M} \otimes \mathbf{n} : \mathbf{C}\rangle - \langle \mathbf{C} : \mathbf{n} \otimes \mathbf{M} \otimes \mathbf{n} : \mathbf{C}\rangle,$$

$$\mathbf{S}_{\mathrm{eff}}^1 = c_1 \langle \mathbf{C} : \mathbf{n} \otimes \mathbf{M}\rangle \cdot \langle \mathbf{M}\rangle^{-1} \cdot \langle \rho \mathbf{M}\rangle - c_1 \langle \rho \mathbf{C} : \mathbf{n} \otimes \mathbf{M}\rangle,$$

$$\mathbf{S}_{\mathrm{eff}}^2 = -c_1 \langle \rho \mathbf{M}\rangle \cdot \langle \mathbf{M}\rangle^{-1} \cdot \langle \mathbf{M} \otimes \mathbf{n} : \mathbf{C}\rangle + c_1 \langle \rho \mathbf{M} \otimes \mathbf{n} : \mathbf{C}\rangle, \tag{18}$$

$$\rho_{\mathrm{eff}} = \langle \rho\rangle \mathbf{I} - c_1^2 \langle \rho \mathbf{M}\rangle \cdot \langle \mathbf{M}\rangle^{-1} \cdot \langle \rho \mathbf{M}\rangle + c_1^2 \langle \rho^2 \mathbf{M}\rangle,$$

which couple stress to velocity and momemtum to strain, when $c_1 > 0$.

We note that such coupling is the counterpart of opto-magnetic coupling in time-modulated electromagnetic media within which light experiences a Fresnel drag [8]. Fresnel drag after Augustin Fresnel, who in 1818 put forward the aether drag hypothesis: a moving fluid appears to drag light along so that light traveling in opposite directions to the fluid flow would have different velocities [29]. Its extra velocity was related to, but not equal to, the velocity of the fluid. Although Fresnel's derivation was flawed, Hippolyte Fizeau measured the drag effect and published in 1851 in the Proceedings of the French Academy of Sciences, nowadays called the Comptes Rendus Physique, an article confirming Fresnel's formula [30]. We thus believe seismic waves propagating in layered soils such as in Figure 8 should experience some similar drag phenomenon due to the ambient noise which acts as a source of time-modulation of the soil. In this case, the Fresnel drag underpins the mechanism of the seismic computer, since this non-reciprocity is an essential ingredient for logical operations, making possible seismic diodes akin electrical diodes, which let electrical currents pass in one direction only and play an essential role in computers. We note in passing some small scale experiments on asymmetric acoustic wave propagation in

unconsolidated granular medium via a nonlinear self demodulation mechanism [31] which could be revisited in light of the effective description using the above equations.

6. Conclusion

We have made a survey of seismic metamaterials, which is an emergent topic beyond electromagnetic metamaterials [32,33], spanning the scales from hundredths of nanometers to tenths of meters [34]. We have revisited some earlier work [1,2], which initiated this fast growing field, and we further described some fortuitous seismic metamaterials from the past (Roman theaters), some natural seismic metamaterials (forest of trees) of present days and some seismic metamaterial computer that might become a reality in the near future. We have stressed that Willis's equations are a good framework for seismic metamaterials, which can be viewed as a mechanical counterpart of time modulated electromagnetic media experiencing some Fresnel drag [8] induced in the present case by seismic ambient noise. This non reciprocity associated with the Fresnel drag can serve to achieve some seismic diodes, and so some logical operations with seismic computers.

Before we conclude this perspective article, we would like to point out an earlier work [35] that unveiled theoretically and experimentally for kHz Rayleigh waves in the Bragg regime some elastic stop bands properties: attenuation of Rayleigh waves was observed in a marble quarry by drilling cylindrical holes arranged in honeycomb and triangular lattices. We further note the theoretical and experimental observation of subwavelength stop bands for MHz Rayleigh waves propagating within an array of nickel pillars grown on a lithium niobate substrate [36]. In our opinion, these two seminal works that predate the area of seismic metamaterials have touched upon the essence of the wave physics at work in large scale mechanical metamaterials: control of surface seismic waves in the Bragg [1,35,37,38] and subwavelength [2,21,36,39–41] regimes. In all fairness, seismologists and earthquake engineers had already noted 40 years ago the effect of soil roughness on the propagation of seismic waves [42]. Of course, shielding and damping of surface seismic waves thanks to stop band properties does not tell all the story of seismic metamaterials, as our team has theoretically and experimentally demonstrated that one can actually focus such waves via negative refraction [2] through a tilted array of boreholes in a sedimentary soil. In fact, the earthquake engineer could arrange boreholes or concrete columns in soil in many ways, for instance in a concentric fashion to achieve a seismic cloak, and some numerical simulations show encouraging results in this direction [43], using some effective medium approach based on Willis's equations. This work takes a new dimension thanks to the concept of time-modulated media. Our group has actually proposed to scale up further the design of seismic cloaks in order to achieve some self-protection for cities [44]. This might seem like a far-fetched concept, but we recall here that geophysicists and civil engineers have already observed theoretically and numerically site-city interactions [20,45–50].

Finally, we would like to conclude this review and perspective article on seismic metamaterials by the proposal that one might be able to further extend ideas rooted in the physics of electromagnetic metamaterials to control, harvest and redirect not only seismic ambient noise but also the powerful energy released near seismic faults during metric sliding mechanism along fault plan. The Figure 9 shows the cumulative displacement (130 m) at San Andreas fault after several earthquakes occured during the last millennia. For an illustrative example of an earthquake of magnitude 4, seismic energy radiated at a fault with similar characteristics can be estimated to be in the order of $M_0 = 2.6 \times 10^{10}$ J (i.e. 26,000 MJ) for a surface of the fault about 1.2×10^6 m $\times 3.5 \times 10^{-2}$ m $= 4.2 \times 10^4$ m^2 (so 42,000 m^2), in a rock of shear modulus $G = 30,000$ MPa. However, a word of caution would be in order as the propagated seismic energy computed from the Gutenberg–Richter formulas [51] would be much smaller. Last, but not least, this article benefited from scientific interactions with colleagues.
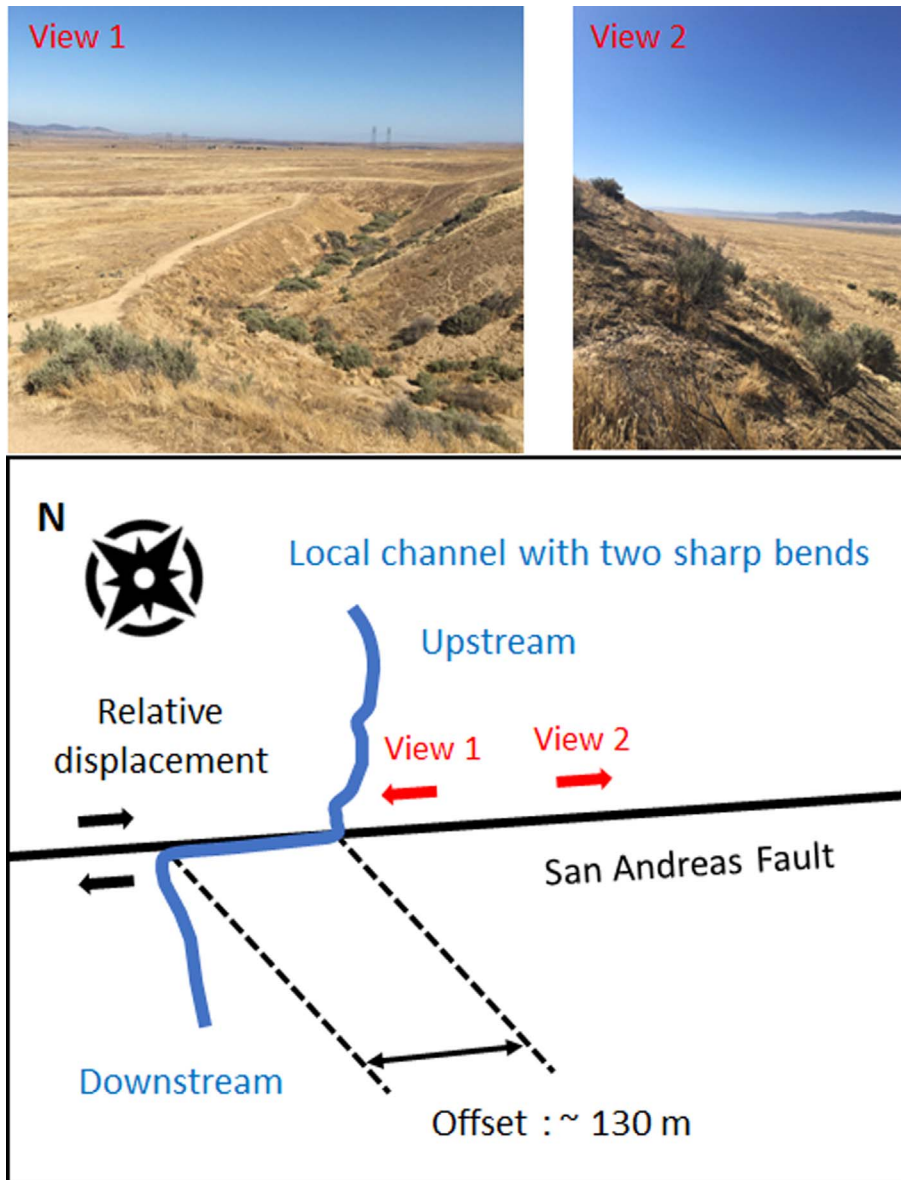
Figure 9. Wallace Creek, Carizo Plain (California, USA). Channel with sharp bends. The upstream half of the channel doesn't line up with its downstream half (upper left panel) because the San Andreas strike-slip fault has been slided (sismo-geological top-view figure). The two tectonic blocks slide past one another. The San Andreas Fault is a right lateral fault (upper right panel). Photo credits: S. Brûlé. From Wallace Creek Interpretive Trail-A geological guide to the San Andreas Fault at Wallace Creek (Southern California Earthquake Center, U.S. Geological Survey, California Institute of Technology and Bureau of Land Management).

References

[1] S. Brûlé, E. Javelaud, S. Enoch, S. Guenneau, "Experiments on seismic metamaterials: molding surface waves", *Phys. Rev. Lett.* **112** (2014), article no. 133901.

[2] S. Brûlé, E. Javelaud, S. Enoch, S. Guenneau, "Flat lens for seismic waves", *Sci. Rep.* **7** (2017), article no. 18066.

[3] S. Brûlé, C. Deprez, C. Fernandez, M. Givry, K. Manchuel, G. Mendoza, B. Richard, C. Taylor, "Report of the post-seismic mission on the mexico earthquake of september 19th, 20017", Tech. report, Association Française du Génie Parasismique (AFPS), 2017.

[4] S. Brûlé, S. Enoch, S. Guenneau, "Role of nanophotonics in the birth of seismic megastructures", *Nanophotonics* **8** (2019), p. 1591-1605.

[5] H. Nassar, X. Xu, A. Norris, G. Huang, "Modulated phononic crystals: non-reciprocal wave propagation and willis materials", *J. Mech. Phys. Solids* **101** (2017), p. 10-29.

[6] J. Willis, "Variational principles for dynamic problems in inhomogeneous elastic media", *Wave Motion* **3** (1981), p. 1-11.

[7] Y. Liu, S. Guenneau, B. Gralak, "Artificial dispersion via high-order homogenization: magnetoelectric coupling and magnetism from dielectric layers", *Proc. R. Soc. Lond. A* **469** (2013), article no. 20130240.

[8] P. Huidobro, E. Galiffi, S. Guenneau, R. Craster, J. Pendry, "Fresnel drag in space-time modulated metamaterials", *Proc. Natl Acad. Sci. USA* **116** (2019), p. 24943-24948.

[9] A. Silva, F. Monticone, G. Castaldi, V. Galdi, A. Alu, N. Engheta, "Performing mathematical operations with metamaterials", *Science* **343** (2014), p. 160-163.

[10] N. Estakhri, B. Edwards, N. Engheta, "Inverse-designed metastructures that solve equations", *Science* **22** (2019), p. 1333-1338.

[11] S. Brûlé, S. Enoch, S. Guenneau, "Sols structurés sous sollicitation dynamique : des métamatériaux en géotechnique", *Rev. Fr. Geotech.* **151** (2017), p. 4.

[12] G. Dupont, O. Kimmoun, B. Molin, S. Guenneau, S. Enoch, "Numerical and experimental study of an invisibility carpet in a water channel", *Phys. Rev. E* **91** (2015), article no. 023010.

[13] M. Farhat, S. Enoch, S. Guenneau, A. Movchan, "Broadband cylindrical acoustic cloak for linear surface waves in a fluid", *Phys. Rev. Lett.* **101** (2008), article no. 134501.

[14] S. Brûlé, S. Enoch, S. Guenneau, "Emergence of seismic metamaterials: current state and future perspectives", *Phys. Lett. A* **384** (2020), article no. 126034.

[15] J. Xu, X. Jiang, N. Fang, E. Georget, R. Abdeddaim, J. Geffrin, M. Farhat, P. Sabouroux, S. Enoch, S. Guenneau, "Molding acoustic, electromagnetic and water waves with a single cloak", *Sci. Rep.* **5** (2015), article no. 10678.

[16] M. Farhat, S. Guenneau, S. Enoch, "Broadband cloaking of bending waves via homogenization of multiply perforated radially symmetric and isotropic thin elastic plates", *Phys. Rev. B* **85** (2012), article no. 020301.

[17] N. Stephen, "On energy harvesting from ambient noise", *J. Sound Vib.* **293** (2006), p. 413-425.

[18] S. Brûlé, S. Enoch, S. Guenneau, "Experimental evidence of auxetic features in seismic metamaterials: Ellipticity of seismic rayleigh waves for subsurface architectured ground with holes", https://arxiv.org/abs/1809.05841, 2018.

[19] S. Brûlé, S. Enoch, S. Guenneau, "On the possibility of seismic rogue waves in very soft soils", 2020, https://arxiv.org/abs/2004.07037.

[20] B. Ungureanu, S. Guenneau, Y. Achaoui, A. Diatta, M. Farhat, H. Hutridurga, R. Craster, S. Enoch, S. Brûlé, "The influence of building interactions on seismic and elastic body waves", *EPJ Appl. Metamater.* **6** (2019), p. 18.

[21] A. Colombi, P. Roux, S. Guenneau, P. Gueguen, R. Craster, "Forests as a natural seismic metamaterial: Rayleigh wave bandgaps induced by local resonances", *Sci. Rep.* **6** (2016), article no. 19238.

[22] A. Colombi, D. Colquitt, P. Roux, S. Guenneau, R. Craster, "A seismic metamaterial: the resonant metawedge", *Sci. Rep.* **6** (2016), article no. 27717.

[23] K. Tsakmakidis, A. Boardman, O. Hess, "Trapped rainbow storage of light in metamaterials", *Nature* **450** (2007), p. 397.

[24] A. Maurel, J. Marigo, K. Pham, S. Guenneau, "Conversion of love waves in a forest of trees", *Phys. Rev. B* **98** (2018), article no. 134311.

[25] J. D. Ponti, A. Colombi, R. Ardito, F. Braghin, A. Corigliano, R. Craster, "Graded metasurface for enhanced sensing and energy harvesting", *New J. Phys.* **22** (2020), article no. 013013.

[26] P. Vitruvius, *Ten Books on Architecture. Vol. 15*, Cambridge University Press, New York, 1999.

[27] A. B. Clymer, "The mechanical analog computers of Hannibal Ford and William Newell", *IEEE Ann. Hist. Comput.* **15** (1993), p. 19-34.

[28] K. Lurie, *An Introduction to the Mathematical Theory of Dynamic Materials*, Springer, New York, 2007.

[29] A. Fresnel, "Lettre d'augustin fresnel a francois arago sur l'influence du mouvement terrestre dans quelques phenomenes d'optique", *Ann. Chem. Phys.* **9** (1818), p. 57-67.

[30] H. Fizeau, "Sur les hypotheses relatives a l'ether lumineux", *C. R. Acad. Sci.* **33** (1851), p. 349-355.

[31] T. Devaux, V. Tournat, O. Richoux, V. Pagneux, "Asymmetric acoustic propagation of wave packets via the self-demodulation effect", *Phys. Rev. Lett.* **115** (2015), article no. 234301.

[32] M. Kadic, T. Buckmann, R. Schittny, M. Wegener, "Metamaterials beyond electromagnetism", *Rep. Prog. Phys.* **76** (2013), article no. 126501.

[33] B. Ungureanu, Y. Achaoui, S. Enoch, S. Brûlé, S. Guenneau, "Auxetic-like metamaterials as novel earthquake protections", *EPJ Appl. Metamater.* **2015** (2016), p. 17.

[34] R. Aznavourian, T. Puvirajesinghe, S. Brûlé, S. Enoch, S. Guenneau, "Spanning the scales of mechanical metamaterials using time domain simulations in transformed crystals, graphene flakes and structured soils", *J. Phys. Condens. Matter* **29** (2017), article no. 433004.

[35] F. Meseguer, M. Holgado, D. Caballero, N. Benaches, J. Sanchez-Dehesa, C. Lopez, J. Llinares, "Rayleigh-wave attenuation by a semi-infinite two-dimensional elastic-bandgap", *Phys. Rev. B* **59** (1999), article no. 12169.

[36] Y. Achaoui, A. Khelif, S. Benchabane, L. Robert, V. Laude, "Experimental observation of locally-resonant and bragg band gaps for surface guided waves in a phononic crystal of pillars", *Phys. Rev. B* **83** (2011), article no. 104201.

[37] M. Miniaci, A. Krushynska, F. Bosia, N. Pugno, "Large scale mechanical metamaterials as seismic shields", *New J. Phys.* **18** (2016), article no. 083041.

[38] Y. Achaoui, T. Antonakakis, S. Brûlé, R. Craster, S. Enoch, S. Guenneau, "Clamped seismic metamaterials: ultra-low frequency stop bands", *New J. Phys.* **19** (2017), article no. 063022.

[39] A. Palermo, S. Krödel, K. H. Matlack, R. Zaccherini, V. K. Dertimanis, E. N. Chatzi, A. Marzani, C. Daraio, "Hybridization of guided surface acoustic modes in unconsolidated granular media by a resonant metasurface", *Phys. Rev. Appl.* **9** (2018), article no. 054026.

[40] M. Lott, P. Roux, S. Garambois, P. Gueguen, A. Colombi, "Evidence of metamaterial physics at the geophysics scale: the metaforet experiment", *Geophys. J. Int.* **220** (2020), p. 1330-1339.

[41] D. Mu, H. Shu, L. Zhao, S. An, "A review of research on seismic metamaterials", *Adv. Eng. Mater.* **22** (2020), article no. e1901148.

[42] H. Wong, M. Trifunac, B. Westermo, "Effects of surface and subsurface irregularities on the amplitude of monochromatic waves", *Bull. Seismol. Soc. Am.* **67** (1977), p. 353-368.

[43] A. Diatta, Y. Achaoui, S. Brûlé, S. Enoch, S. Guenneau, "Control of Rayleigh-like waves in thick plate willis metamaterials", *AIP Adv.* **6** (2016), article no. 121707.

[44] S. Brûlé, B. Ungureanu, Y. Achaoui, R. Aznavourian, T. Antonakakis, R. Craster, S. Enoch, S. Guenneau, "Metamaterial-like transformed urbanism", *Innov. Infrastruct. Solut.* **2** (2017), p. 20.

[45] A. Wirgin, P. Bard, "Effects of buildings on the duration and amplitude of ground motion in mexico city", *Bull. Seismol. Soc. Am.* **86** (1996), p. 914-920.

[46] J. Semblat, A. Duval, P. Dangla, "Numerical analysis of seismic wave amplification in nice (france) and comparisons with experiments", *Soil Dyn. Earthq. Eng.* **19** (2000), p. 347-362.

[47] D. Clouteau, D. Aubry, "Modification of the ground motion in dense urban areas", *J. Comput. Acoust.* **9** (2001), p. 1659-1675.

[48] P. Gueguen, P. Bard, F. Chavez-Garcia, "Site-city seismic interaction in mexico city-like environments: an analytical study", *Bull. Seismol. Soc. Am.* **92** (2002), p. 794-811.

[49] C. Boutin, P. Roussillon, "Assessment of the urbanization effect on seismic response", *Bull. Seismol. Soc. Am.* **94** (2004), p. 251-268.

[50] M. Kham, J. Semblat, P. Bard, P. Dangla, "Seismic site-city interaction: main governing phenomena through simplified numerical models", *Bull. Seismol. Soc. Am.* **96** (2006), p. 1934-1951.

[51] B. Gutenberg, C. Richter, "Magnitude and energy of earthquakes", *Ann. Geofis.* **9** (1956), p. 1-15.